5

Nanowire Applications: Thermoelectric Cooling and Energy Harvesting

Gang Zhang
Key Laboratory for the Physics and Chemistry of Nanodevices and Department of Electronics, Peking University
China

1. Introduction

Recently, thermoelectric materials have attracted extensive attention again. This is primarily due to the increasing awareness of the deleterious effect of global warming on the planet's environment, a renewed requirement for long-life electrical power sources, and the increasing miniaturization of electronic circuits and sensors. Thermoelectrics is able to make a contribution to meet the requirements of all the above activities. Moreover, the advent of nanotechnology has had a dramatic effect on thermoelectric material development and has resulted in the syntheses of nanostructured materials whose thermoelectric properties surpass the best performance of its bulk counter, such as Silicon nanowires (SiNWs). (Boukai et al., 2008; Hochbaum et al., 2008) SiNWs are appealing choice in the novel nano-scale TE materials because of their small sizes and ideal interface compatibility with conventional Si-based technology. For a good thermoelectric material, the material must have a high figure of merit (ZT), which is proportional to the Seebeck coefficient (S), electrical conductivity, and absolute temperature, but inversely proportional to thermal conductivity. In order to make materials that are competitive for (commercial) thermoelectric application, the ZT of the material must be larger than three. There are several ways to do this. The first approach is to increase the Seebeck coefficient S. However, for general materials, simply increase S will lead to a simultaneous decrease in electrical conductivity. The second approach is to increase the electrical conductivity. This has also proven to be ineffective, because electrons are also carriers of heat and an increase in electrical conductivity will also lead to an increase in the thermal conductivity. The ideal case is to reduce the thermal conductivity without affecting the electrical conductivity. It is possible to achieve this in SiNWs. In SiNWs, the electrical conductivity and electron contribution to Seebeck coefficient are similar to those of bulk silicon, but exhibit 100-fold reduction in thermal conductivity, showing that the electrical and thermal conductivities are decoupled. Recent experiments have provided direct evidence that an approximately 100-fold improvement of the ZT values over bulk Si are achieved in SiNW over a broad temperature range. (Boukai et al., 2008; Hochbaum et al., 2008) This large increase of ZT is contributed by the decrease of thermal conductivity. SiNWs have attracted broad interests in recently years due to their fascinating potential applications. Extensive investigations have been carried out on the synthesis, properties and applications of SiNWs. Experimental

technology has been developed to control the growth of SiNWs not only in various growth orientations, but also with various shapes of transverse cross section including rectangle (square), hexagon (rough circle), and triangle. A large number of theoretical and experimental works have been done to explore the properties and applications of these nano wires. Due to the limit of space, here we only address the most fundamental aspects of thermoelectric in nanowires. For the comprehensive review of nanoscale thermal conductivity, please refer to these articles (Cahill et al., 2002; G. Zhang & B. Li, 2010). However, to be self-consistent, we will also give a brief summary about the anomalous thermal conduction and diffusion in one-dimensional nano materials. These results are helpful in understanding the phonon transport in nanowires. In this chapter, it provides an update of recent developments and serves both as an authoritative reference text on thermoelectric property of nanowires for the professional scientist and engineer, and as a source of general information on thermoelectric application for the well-informed layman. This chapter is review type and arranged in eight sections, entitled Introduction; Thermal Conduction in Low-Dimensional Systems; Impact of doping on thermal conductivity of NWs; Effect of surface roughness on phonon transport; Reduction of thermal conductivity by surface scattering; Thermoelectric Property of SiNWs; Realization of SiNW based On-Chip Coolers and Conclusion.

2. Thermal conduction in low-dimensional systems

In recent years, different models and theories have been proposed to study the phonon transport mechanism in low dimensional system. The physical connection between energy diffusion and thermal conductivity has been demonstrated theoretically. (B. Li et al., 2005) For instance, when phonon transports diffusively, which is what we have in bulk material, the thermal conductivity is a size-independent constant. However, in the ballistic transport region, the thermal conductivity of the system increases with the system size, which is the case for ideal One-Dimensional harmonic lattice. Low dimensional nanostructures such as nanowires and nanotubes provide a test bed for these new theories.

Regardless of the specific application, it is obvious that the systematic applications of nano materials will be greatly accelerated by a detailed understanding of their material property. Thermal property in nanostructures differs significantly from that in macrostructures because the characteristic length scales of phonon are comparable to the characteristic length of nanostructures. In bulk materials, the optical phonon modes contribute little to heat flux. However, in nano system, optical phonon (short wavelength) also plays a major role to the heat flux.

A large variety of studies on thermal conductivity of nano materials have been undertaken in the past decade, and quite unexpected phenomena have been observed. This chapter is to address the most important aspects of thermal conduction and thermoelectric property in low dimensional nano materials, of particular focus on semiconducting nanowires. For a comprehensive review of nanoscale thermal conductivity, please refer to these articles. (Cahill et al., 2002; G. Zhang & B. Li, 2010)

2.1 Thermal conduction in nanotubes

Carbon nanotube (CNT) is one of the promising nanoscale materials discovered in 1990's. (Iijima, 1991) It has many exceptional physical and chemical properties. Depending on its

chirality and diameter, the nanotube can be either metallic or semiconducting. At room temperature, the electronic resistivity is about 10^{-4}–10^{-3} Ω cm for the metallic nanotubes, while the resistivity is about 10 Ω cm for semiconducting tubes. By combining metallic and semiconducting CNTs, the whole span of electronic components can be embodied in nanotubes. Actually, CNTs are ranked among the best electron field emitters that are now available.

In the past few years, there has been some experimental works on the heat conduction of CNTs. The thermal conductivity of a single CNT was found to be larger than 3000 W/mK at room temperature. (Kim et al., 2001) In addition to the experimental activity, there are also many theoretical studies on heat conduction of CNTs. It was found that at room temperature, thermal conductivity of CNTs is about 6600 W/mK. (Berber et al., 2000) Yamamoto *et al.* have demonstrated that even for the metallic nanotubes, the electrons give some but limited contributions to thermal conductivity at very low temperature (colse to 0 K), and this part decreases quickly with temperature increasing. (Yamamoto et al., 2004) More important, it is found that thermal conductivity of CNT κ diverges with length as a power law: $\kappa \propto L^{\beta}$, with the exponents β is between 0.12 to 0.4 (G. Zhang & B. Li, 2005) and between 0.11 to 0.32 (Maruyama, 2002). This length dependent thermal conductivity can be understood from the vibrational energy diffusion in SWNT.

2.2 Thermal conduction in nanowires

In addition to CNTs, Silicon nanowires (SiNWs) have attracted a great attention in recent years because of their potential applications in many areas including biosensor (Cui et al., 2001), electronic device (Xiang et al., 2006) and solar PVs (J. Li et al., 2009). SiNWs are appealing choice because of their ideal interface compatibility with conventional Si-based devices.

Due to the size effect and high surface to volume ratio, the thermal conduction properties of silicon nanostructures differ substantially from those of bulk materials. Volz and Chen (Volz & G. Chen, 1999; 2000) have found that the thermal conductivity of individual silicon nanowires is more than 2 orders of magnitude lower than the bulk value. Li *et al.* (D. Li et al., 2003) have also reported a significant reduction of thermal conductivity in silicon nanowires compared to the thermal conductivity in bulk silicon experimentally. The reduction in thermal conductivity is due to the following two factors. Firstly, the low frequency phonons, whose wave lengths are longer than the scale of nanowire, cannot survive in nanowire. Therefore, the low frequency contribution to thermal conductivity is largely reduced. Secondly, because of the large surface to volume ratio, the boundary scattering in NW is greatly significant.

More experimental and theoretical activities have been inspired to do further in this direction, including the theoretical prediction of thermal conductivity of Ge nanowires, molecular dynamics simulation of SiGe NWs, and experimental growth of the isotopic doped SiNWs. The low temperature (<2K) thermal conductance of individual suspended SiNWs was measured by Bourgeois *et al.* (Bourgeois et al., 2007) And the pure phonon confinement effect has been observed in germanium nanowires by measurement of Raman spectra. (X, Wang et al., 2007)

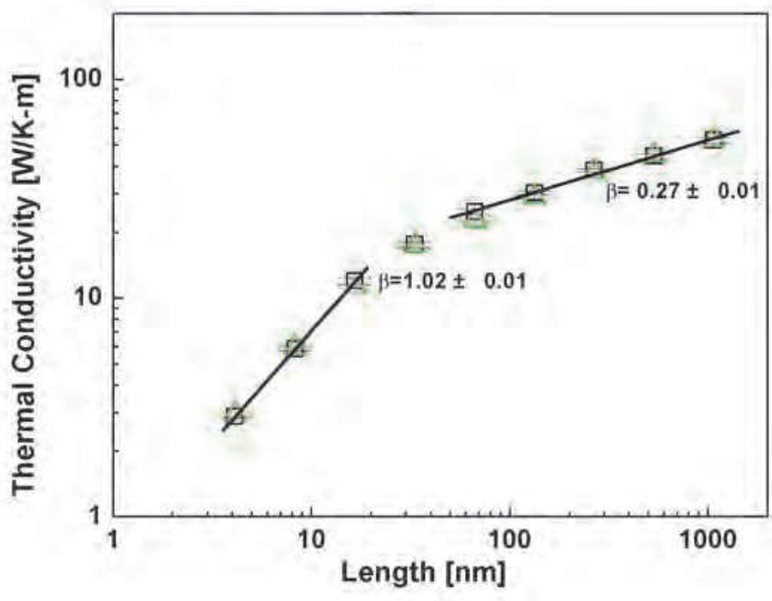

Fig. 1. The thermal conductivity of SiNWs vs longitude length

The similar length dependent thermal conductivity was also observed in SiNWs by using NEMD simulation. (N. Yang et al., 2010) As shown in Fig. 1, it is obvious that the thermal conductivity increases with the length as, $\kappa \propto L^{\beta}$, even when the wire length is as long as 1.1 μm. By using the phonon relaxation time (~10 ps) in SiNWs (Volz & G. Chen, 1999), and the group velocity of phonon as 6400 m/s (N. Yang et al., 2010), the mean free path λ is about 60nm. The maximum SiNW length (1.1 μm) in Fig. 1 is obviously much longer than the phonon mean free path of SiNW. Traditionally, it is well known that in macroscopic systems, the thermal conductivity is a constant when system scale $L >> \lambda$. However, the NEMD results demonstrated that in SiNWs, thermal conductivity is no longer a constant even when the length is obviously longer than the traditionally mean free path.

Moreover, it is obvious that the length dependence of thermal conductivity is different in different length regimes. At room temperature, when SiNW length is less than mean free path (about 60 nm), the thermal conductivity increases with the length linearly ($\beta \approx 1$). For the longer wire (L > 60 nm), the diverged exponent β reduces to about 0.27. The dependence of β on NW length can be understood from the picture of phonon coupling. There is weak interaction among phonons when the length of SiNW is shorter than mean free path. So the phonons transport ballistically, and $\beta \approx 1$. However, when the length of SiNW is longer than the mean free path, phonon-phonon scattering dominates the process of phonon transport and the phonon cannot flow ballistically. Thus the diverged exponent β reduces from 1 to 0.27.

Then let us turn to the energy diffusion process in SiNWs. To study the energy diffusion process, the SiNW is first thermalized to a temperature T, then a heat pulse (a packet of energy) is excited in the middle of the wire and its spreads along the wire was recorded. To suppress statistical fluctuations, an average over 10^3 realizations is performed. The details of the numerical calculation can be found in (N. Yang et al., 2010). Based on billiard gas

channel models, Li and Wang (B. Li & J. Wang, 2003) proposed a phenomenologically formula that connect anomalous heat conduction with the anomalous diffusion of heat carrier, namely, $\beta = 2 - 2/\alpha$. This connection indicates that only when the heat carrier undergoes normal diffusion like in the bulk material, the thermal conductivity is independent of system size. In super-diffusion case, $\alpha > 1$, the exponent $\beta > 0$, which means that thermal conductivity diverges with system size, this is the case observed in thermal conductivity of CNTs and SiNWs. In Fig. 2 we show $<\sigma^2(t)>$ versus time in double logarithmic scale, so that the slope of the curve gives the value of α. For the NWs of length of 140 nm, it was obtained $\alpha = 1.15$ at 300 K. With the value of diffusion exponent ($\alpha = 1.15$ at 300 K), one can obtain $\beta = 0.26$ at 300 K, which are very close to those values (0.27) calculated directly from NEMD simulation. These results demonstrate that the super diffusion is responsible for the length dependent thermal conductivity of SiNWs.

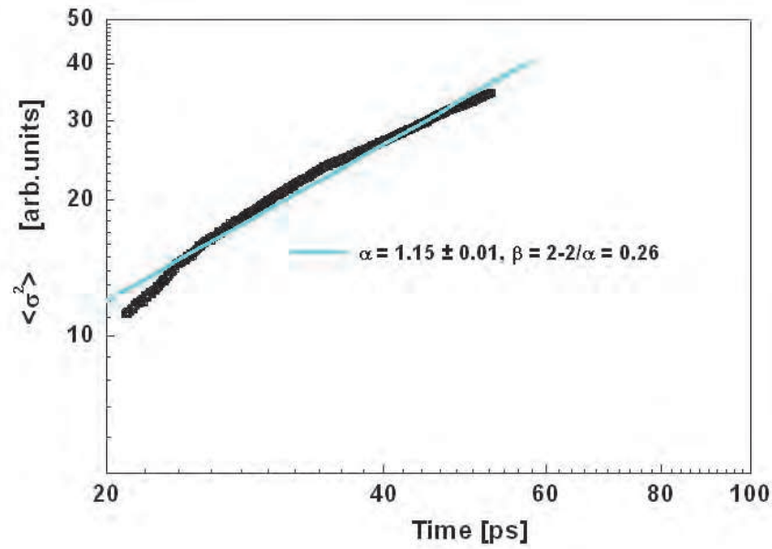

Fig. 2. The behavior of energy diffusion in SiNW at room temperature. The length of SiNW is 140 nm.

3. Impact of doping on thermal conductivity of NWs

Although the thermal conductivity of SiNWs is lower than that of the bulk silicon, it is still larger than the reported ultralow thermal conductivity (0.05 W/m-K) found in layered materials. So it is indispensable to reduce the thermal conductivity of SiNWs further in order to achieve higher thermoelectric performance. Actually, real materials can have natural defects and doping in the process of fabrication. The doping of isotope and/or other atoms have played key roles in some of the most important problems of materials, such as elastic, and field emission properties. Since the phonon frequency depends on mass, the isotopic doping can lead to increased phonon scattering. Thus, natural SiNW always contain a significant number of scattering centers leading to localization of some phonon modes and reduces thermal conductivity. By using molecular dynamics simulations, Yang *et al.* (N. Yang et al., 2008) have proposed one approach which is to dope SiNWs with isotope

impurity randomly for reduction of thermal conductivity of SiNWs. In silicon isotopes, ^{28}Si is with the highest natural abundance (*92%*), then ^{29}Si and ^{30}Si with *5%* and *3%* respectively. Here the effect of doping ^{29}Si to ^{28}Si NWs are shown.

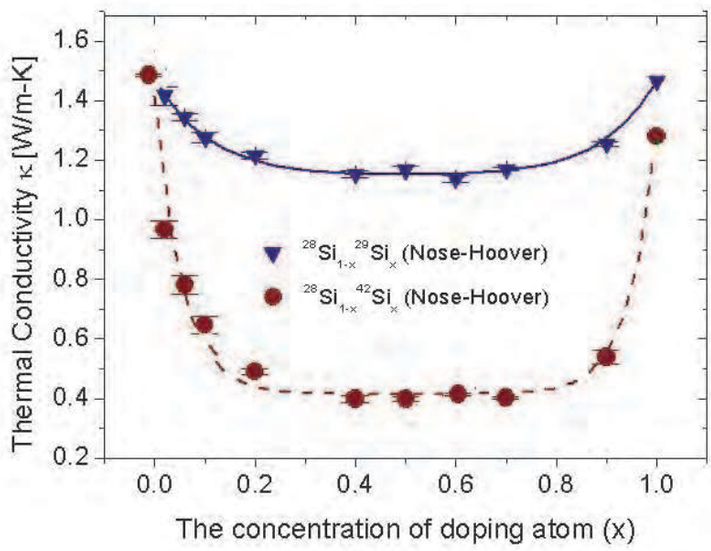

Fig. 3. Thermal conductivity of SiNWs versus the percentage of randomly doping isotope atoms (^{42}Si and ^{29}Si) at 300K.

The curve of thermal conductivity first reach a minimum and then increases as the percentage of isotope impurity atoms changes from 0 to 100%. At low isotopic percentage, the small ratio of impurity atoms can induce large reduction on conductivity. Contrast to the high sensitivity at the two ends, the thermal conductivity versus isotopic concentration curves are almost flat at the center part as show in Fig. 3, where the value of thermal conductivity is only 77% (^{29}Si doping) of that of pure ^{28}Si NW. The calculated thermal conductivity of SiNW with natural isotopic abundance, 5% ^{29}Si and 3% ^{30}Si is around 86% of pure ^{28}Si NW, which reduction (14%) is higher than the experimental results in bulk Si, which is about 10% reduction.

In addition to the disorder doping, it has been shown that superlattices are efficient structures to get ultra low thermal conductivity. The isotopic-superlattice (IS) is a good one to reduce the thermal conductivity without destroying the stability. The thermal conductivity of IS structured NWs which consists of alternating ^{28}Si/^{29}Si layers along the longitudinal direction are shown in Fig. 4. As expected, the thermal conductivity decreases as the period length decreases, which means the number of interface increases. The thermal conductivity reaches a minimum when the period length is *1.09* nm. This is consistent with the fact that increasing number of interface will enhance the interface scattering, and results to the reduction of the thermal conductivity. With the period length smaller than *1.09* nm, the thermal conductivity increases rapidly as the period length decreases. This anomalous superlattice dependence of thermal conductivity can be understood from the phonon density of states (DOS). When period length is *2.17* nm, there is an obvious mismatch in the DOS spectra, both at low frequency band and high frequency band, results in very low thermal conductivity. On the contrary, the DOS spectra overlap perfectly for IS structured

SiNW whose period length is *0.27* nm. The good match in the DOS comes from the collective vibrations of different mass layers which is harder to be built in longer superlattice period structures. The match/mismatch of the DOS spectra between the different mass layers controls the heat current.

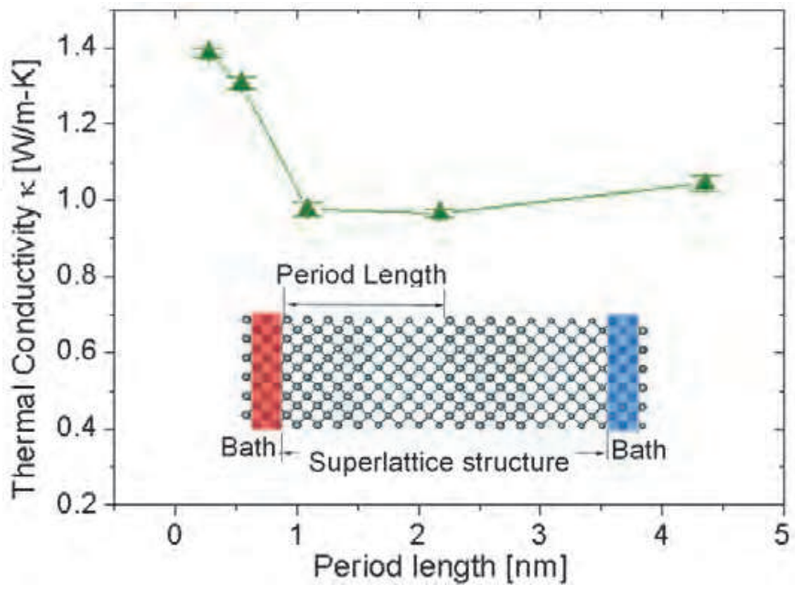

Fig. 4. Thermal conductivity of the superlattice SiNWs versus the period length at 300 K.

It is worth to point out that the growth of isotopically controlled silicon nanowires by the vapor-liquid-solid mechanism has been done recently. (Moutanabbir et al., 2009) The growth is accomplished by using silane precursors $^{28}SiH_4$, $^{29}SiH_4$ and $^{30}SiH_4$ synthesized from SiF_4 isotopically enriched in a centrifugal setup. And the effect of isotope doping on Si-Si LO phonon has also been investigated. The corresponding experimental measurement of thermal conductivity is on-going.

Moreover, Silicon and Germanium can form a continuous series of substitutional solid, $Si_{1-x}Ge_x$ over the entire compositional range of $0 \le x \le 1$. These semiconductor alloys offer a continuously variable system with a wide range of crystal lattices and band gaps, leading to various electrical property. Single crystalline $Si_{1-x}Ge_x$ NWs have been successfully grown. (J-E. Yang et al., 2006) Those composite nanocrystals constitute a new class of semiconductor materials with unique chemical and physical properties which are not possible in single-component compounds. The tenability of those properties makes this kind of semiconductor systems very attractive for industrial application. In spite of an increasing number of works devoted to the electronic and optical properties, very little has done for thermal conductivity of $Si_{1-x}Ge_x$ NW.

Here we address the non-equilibrium molecular dynamics (NEMD) calculated thermal conductivity of $Si_{1-x}Ge_x$ NWs with x changing from 0 to 1. (J. Chen et al., 2009) In NEMD, to derive the force term, Stillinger-Weber (SW) potential (Stillinger & Weber, 1985) is used for Si and Ge. SW potential consists of a two-body term and a three-body term that can stabilize the diamond structure of silicon and germanium. The two-body interaction can be described as:

$$v_2(r_{ij}) = \varepsilon f_2(r_{ij} / \sigma), \tag{1}$$

$$f_2(r) = A(Br^{-p} - r^{-q})exp[(r-a)^{-1}], (r < a) \tag{2}$$

where r_{ij} is the inter atomic distance, A, B, p, q, ε and σ are potential parameters, and a is the potential cutoff distance above which no interaction occurs. The three-body interaction is:

$$v_3(\mathbf{r}_i, \mathbf{r}_j, \mathbf{r}_k) = \varepsilon f_3(\mathbf{r}_i / \sigma, \mathbf{r}_j / \sigma, \mathbf{r}_k / \sigma),$$

$$f_3(\mathbf{r}_i, \mathbf{r}_j, \mathbf{r}_k) = h(r_{ij}, r_{ik}, \theta_{jik}) + h(r_{ji}, r_{jk}, \theta_{ijk}) + h(r_{ki}, r_{kj}, \theta_{ikj}), \tag{3}$$

$$h(r_{ij}, r_{ik}, \theta_{jik}) = \lambda \exp[\gamma(r_{ij} - a)^{-1} + \gamma(r_{ik} - a)^{-1}] \times (\cos\theta_{jik} + 1/3)^2,$$

where λ and γ are potential parameters, and θ_{ijk} is the angle between r_{ij} and r_{ik}. The parameters of Si-Ge interactions are taken to be the arithmetic average of Si and Ge parameters for σ_{Si-Ge}, and the geometric average for λ_{Si-Ge} and ε_{Si-Ge}.
According to the Boltzmann distribution, the temperature T_{MD} in MD simulation, is calculated from the kinetic energy of atoms as:

$$\langle E_k \rangle = \frac{1}{2}\sum_{i=1}^{N} m_i v_i^2 = \frac{3}{2} N k_B T_{MD}, \tag{4}$$

where <E_k>is the mean kinetic energy, v_i is the velocity of atom i, m is the atomic mass, N is the number of particles in the systems, and k_B is the Boltzmann constant. However, Eq. (4) is valid only when T>>T_D, where T_D is the Debye temperature. Therefore, if the system is simulated at a MD temperature below the Debye temperature (T_D=645K for Si), a quantum correction to both MD temperature and thermal conductivity should be carried out. According to the equipartition theorem, the system energy is twice the kinetic energy. So we can write the equality of phonon energy as:

$$3Nk_B T_{MD} = \int_0^{\omega_D} D(\omega) n(\omega, T) \hbar\omega d\omega, \tag{5}$$

where ω is the phonon frequency, $D(\omega)$ is the density of states, $n(\omega, T)$ is the phonon occupation number given by the Bose-Einstein distribution, and ω_D is the Debye frequency. The real temperature T can be deduced from the MD temperature T_{MD} by this relation. Correspondingly, the "real" thermal conductivity is rescaled by

$$k = k_{MD} \frac{|\nabla T_{MD}|}{|\nabla T|} = k_{MD} \frac{\partial T_{MD}}{\partial T}. \tag{6}$$

When T_{MD} is at room temperature, 300K, the rescale rate (a=$\partial T_{MD}/\partial T$) α=0.91 for silicon, which gives a quite small quantum correction effect on thermal conductivity.
Figure 5 shows the thermal conductivity κ versus Ge content x at room temperature. The thermal conductivity of pure SiNW calculated is 3.18W/m-K. The lowest κ is 0.59W/m-K, which is 18% of that of pure SiNW. At the two ends of the curves, the thermal conductivity

shows a very sensitive dependence on x and follows an exponential decay, which is caused by the localization of high frequency phonons by the impurity. It is quite interesting that with only 5% Ge atoms ($Si_{0.95}Ge_{0.05}$ NW), its thermal conductivity can be reduced 50%.

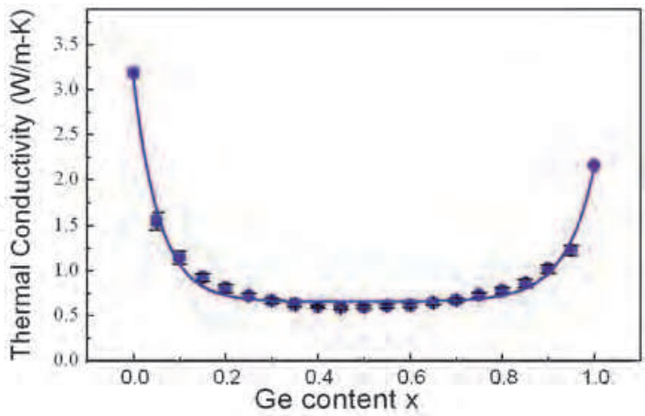

Fig. 5. The thermal conductivity κ versus x at T=300K. The blue circles are the average values of the simulation results, and the solid curve is the best fitting to the formula $\kappa = A_1 e^{-x/B_1} + A_2 e^{-(1-x)/B_2} + C$.

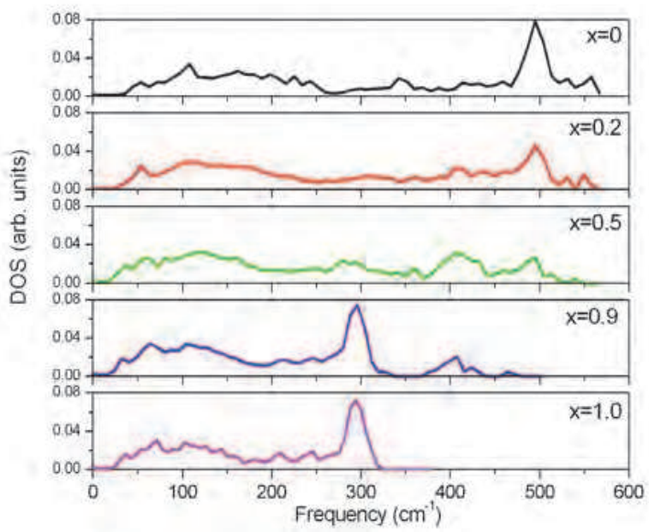

Fig. 6. The representative PDOS for $Si_{1-x}Ge_x$ NWs with $0 \le x \le 1$.

To understand the compositional dependence of thermal conductivity, we show representative phonon density of states (PDOS) of the $Si_{1-x}Ge_x$ NWs in Figure 6. There is significant difference between nano and bulk material in the PDOS, in particular in the high frequency regime. In bulk materials, the optical modes contribute little to heat flux. However, in nano scale system, optical phonon (high frequency) also plays a major contribution to heat flux. For both pure Si NW and pure Ge NW, a significant PDOS peak appears at high frequency range, indicating the main contribution of optical modes to heat flux. However, in the $Si_{1-x}Ge_x$ NWs (0<x<1), as the introduction of disorder scattering, the main PDOS peak at

high frequency range weakens and vanishes with the impurity concentration increasing. In contrast to the strong dependence of high frequency PDOS on x, the low frequency PDOS are almost independent on the composition change. This is consistent with the idea that in nano materials, the high frequency phonons are more sensitivity to the impurity than low frequency phonons (which have long wavelength) do, and the reduction in thermal conductivity mainly comes from the suppressing of high frequency modes. (Che et al., 2000)

4. Effect of surface roughness on phonon transport

It is well known that the thermal conductivity of NW decreases with wire diameter. To calculate the diameter dependent thermal conductivity quantitatively, an analytical formula including the surface scattering and the size confinement effects of phonon transport is proposed by Liang and Li (Liang & B. Li, 2006) to describe the size dependence of thermal conductivity in NWs and other nanoscale structures. In their approach, the phonon-phonon interaction is assumed to increase with size reduction due to the confinement, which causes the decrease of heat conduction. On the other hand, as the size decreases and the surface-volume ratio increases, the large surface/interface scattering, corresponding to certain boundary conditions, has great influence on the transport. Considering the nonequilibrium phonon distribution due to boundary scattering, the effect of the surface roughness with the boundary scattering shows an exponential suppression in the distribution and the conduction. Then, the quantitative formula for the size-dependent thermal conductivity of SiNW is obtained (Liang & B. Li, 2006):

$$\frac{\kappa}{\kappa_b} = p\exp(-\frac{d_0}{D})\left[\exp\left(\frac{-(\alpha-1)}{D/\lambda-1}\right)\right]^{3/2} \tag{7}$$

Here κ is the thermal conductivity of SiNW, κ_b is the thermal conductivity of bulk silicon. The details about this formula can be found in (Liang & B. Li, 2006). This empirical formula gives a quantitative prediction for the size-dependent thermal conductivity. The larger value of p corresponds to the smaller roughness, thus the more probability of specular scattering. Thermal conductivity of Si nanowires from the experiments and the comparison with theoretical predictions from Eq. (7) with suitable parameters p are shown in Fig. 7. The predictions are in good agreements with the experimental results. (D. Li et al., 2003) It is obvious that the phonon thermal conductivity increases with diameter increases remarkably until the diameter is larger than about hundreds nms. This reflects the fact that scattering at the surface introduces diffuse phonon relaxation in the transverse cross section. After the diameter reaches large values, the portion of phonons experiencing boundary scattering becomes much smaller, as a result, the thermal conductivity tends to be constant and is close to the value of bulk silicon. For Si nanowires with diameter of 20–100 nm, p=0.4, reflecting the larger surface roughness of the nanowires in the sample fabrication. This is consistent with the experimental image. (Hochbaum et al., 2008)

Donadio and Galli (Donadio & Galli, 2009) also studied heat transport in SiNWs systematically, by using molecular dynamics simulation, lattice dynamics, and Boltzmann transport equation calculations. It was demonstrated that the disordered surfaces, nonpropagating modes analogous to heat carriers, together with decreased lifetimes of propagating modes are responsible for the reduction of thermal conductivity in SiNWs.

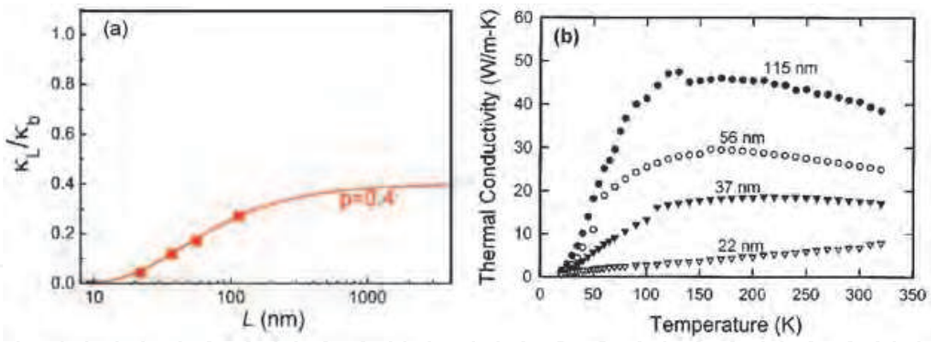

Fig. 7. Size-dependent thermal conductivity of Si nanowires.(a) Comparison of thermal conductivity between theoretical prediction and experimental measurements. The curve is prediction from Eq. 7 and the symbols are experimental results from(D. Li et al., 2003). (b) The experimental temperature dependent thermal conductivity from (D. Li et al., 2003).

5. Reduction of thermal conductivity by surface scattering

Very recently, another mechanism to reduce thermal conductivity by introducing more surface scattering: making SiNWs hollow to create inner surface, i.e. silicon nanotubes (SiNTs) was proposed. (J. Chen et al., 2010) Fig. 8 shows the thermal conductivity of SiNWs and SiNTs versus cross section area at 300K. It is interesting to find that even with a very small hole, the thermal conductivity decreases obviously, from κ_{NW}=12.2±1.4 W/mK to κ_{NT}=8.0±1.1 W/mK. In this case, only a 1% reduction in cross section area induces the reduction of thermal conductivity of 35%. Moreover, with increasing of size of the hole, a linear dependence of thermal conductivity on cross section area is observed. It is clear that for SiNW, thermal conductivity decreases with cross section area decreases. This is because with the increase of size, more and more phonons are excited, which results in the increase of thermal conductivity. So the decrease of cross section area is one origin for the low thermal conductivity of SiNT but not the sole one. We can see that with the same cross section area, thermal conductivity of SiNTs is only about 33% of that of SiNWs. This additional reduction is due to the localization of phonon states on the surface.

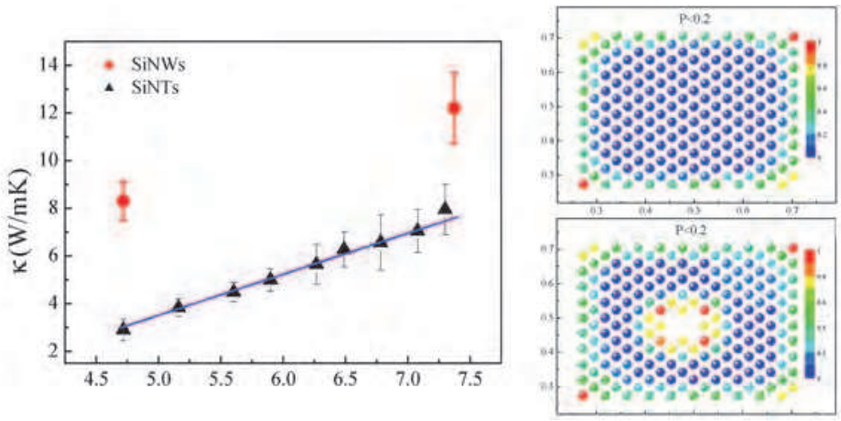

Fig. 8. Left: Thermal conductivity of SiNWs and SiNTs versus cross section area at 300K. Right: Normalized energy distribution on the cross section plane for SiNWs and SiNTs. Here are energy distribution for modes with P<0.2.

To understand the underlying physical mechanism of thermal conductivity reduction in SiNTs, a vibrational eigen-mode analysis on SiNWs and SiNTs was carried out. Mode localization can be quantitatively characterized by the participation ratio P_λ which measures the fraction of atoms participating in a given mode, and effectively indicates the localized modes with O(1/N) and delocalized modes with O(1). Fig. 8 shows the normalized energy distribution on the cross section plane for SiNWs and SiNTs at 300K. The positions of the circles denote different locations on plane. For those localized modes with p-ratio less than 0.2, it is clearly shown that the intensity of localized modes is almost zero in the centre of NW, while with finite value at the boundary. This demonstrates that the localization modes in SiNWs are distributed on the boundary of cross section plane, which corresponds to the outer surface of SiNWs. In addition, due to inner-surface introduced in SiNTs, energy localization also shows up around the hollow region. These results provide direct numerical evidence that localization takes place on the surface region.

Compared with SiNWs, SiNTs have a larger surface area, which corresponds to a higher SVR. As a result, there are more modes localized on the surface, which increases the percentage of the localized modes to the total number of modes. In heat transport, the contribution to thermal conductivity mainly comes from the delocalized modes rather than the localized modes. Due to the enhanced SVR in SiNTs which induces more localized modes, the percentage of delocalized modes decreases, leads to a reduction of thermal conductivity in SiNTs compared with SiNWs. Very recently, the similar SiNT structures have been fabricated experimentally by reductive decomposition of a silicon precursor in an alumina template and ething (Park et al., 2009). Thus SiNTs is a promising thermoelectric material by using reliable fabrication technology.

6. Thermoelectric property of SiNWs

From above sections, it is well established that reduction of thermal conductivity, such as by isotopic doping, is an efficient way to increase the figure of merit ZT. ZT depends on both the phonon and electron transport properties. Thus to maximize the performance of SiNW thermoelectric cooler, it is indispensable to have a comprehensive understanding of the above factors. In this section, we will discuss systematically the impacts of size, isotope concentration and alloy effect on thermoelectric property of SiNW.

By using the density functional derived tight-binding method (DFTB), Shi et al. (L. Shi et al., 2009) have studied the size effect on thermoelectric power factor. The DFTB has high computational efficiency and allows the simulation of bigger systems than conventional density functional theory (DFT) at a reasonable computational time and with similar accuracy. Here the cross section area is ranging from 1 nm^2 to about 18 nm^2. The corresponding diameter D is from 1.7 to 6.1 nm.

It has been shown that electron transport is diffusive in SiNWs longer than 1.4 nm. (Gilbert et al., 2005) Therefore, σ, S and κ_e are evaluated by only elastic scattering processes. The electrical conductivity σ, the electron thermal conductivity κ_e, and the Seebeck coefficient S, are obtained from the electronic structure with the solution of 1-Dimensional Boltzmann transport equation as:

$$\sigma = \Lambda^{(0)}$$
$$\kappa_e = \frac{1}{e^2 T}[\Lambda^{(2)} - \Lambda^{(1)}(\Lambda^{(0)})^{-1}\Lambda^{(1)}]$$
$$S = \frac{1}{eT}(\Lambda^{(0)})^{-1}\Lambda^{(1)} \tag{8}$$
$$A^{(n)} = e^2\tau\frac{2}{m^*}\sum_{E_k}\Delta E\left[\frac{\beta\exp(\beta(E_k-\mu))}{(1+\exp(\beta(E_k-\mu)))^2}\right]D(E_k)E_k(E_k-\mu)^n$$

Here e is the charge of carriers, T is the temperature, E_k is the electron energy, τ is the relaxation time, m* is the effective mass of the charge carrier, μ is the electron chemical potential and $D(E_k)$ is the density of states. The relaxation time τ, is obtained by fitting the calculated mobility to measured electrical conductivity data of SiNW.
The carrier concentration is defined as:

$$n = \int D(E-\mu)\times f(E-\mu)\times dE\,, \tag{9}$$

where $f(E)$ is the Fermi distribution function. In this model, n corresponds to the concentration of charge in a system that is artificially doped by varying the chemical potential while assuming a fixed band structure. With the change in μ, the carrier concentration changes, and induces the corresponding modification in thermoelectric property.
Figure 9(a) and 9(b) show the size effects on σ and S with different electron concentration. The size dependence arises from quantum confinement effect on the electronic band structure of SiNWs. It is obvious that the larger the dimension of the wire the smaller the band gap due to quantum confinement. In contrast to the weak size dependence of electronic conductivity, Seebeck coefficient S decreases with increasing of size remarkably.

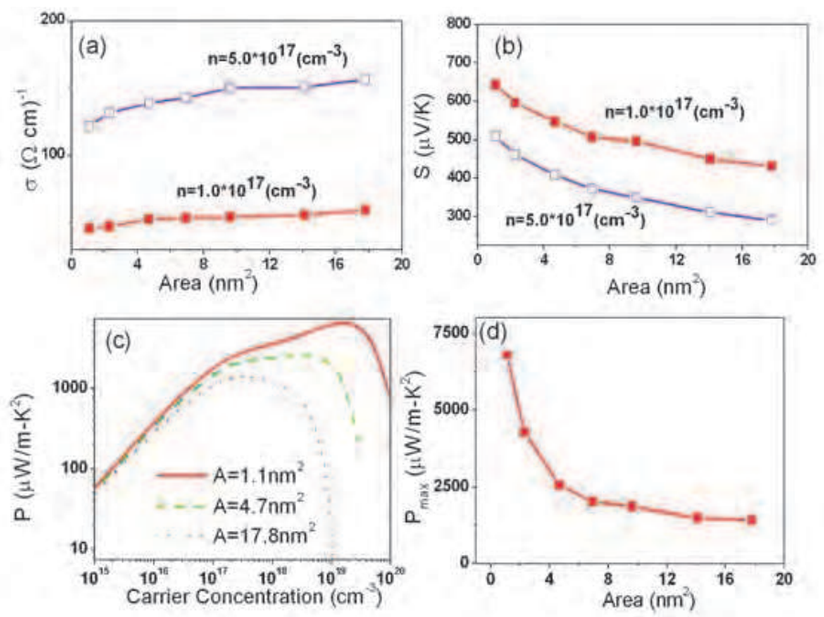

Fig. 9. (a) and (b) Electrical conductivity and S vs cross sectional area with different carrier concentration. (c) Thermal power factor of SiNW vs carrier concentration. (d) Maximum power factor vs cross sectional area.

Besides the electronic band gap, Seebeck coefficient S also depends on the detailed band structure, in which narrow DOS distribution is preferred. (R. Y. Wang et al., 2008) In a bulk material, the continue electron energy levels give a wide distribution of carrier energies. However, the DOS of SiNW differs dramatically from that of bulk silicon. The large numbers of electronic stats in narrow energy ranges can lead to large S. With the transverse dimension increases, the sharp DOS peaks widen and reduces S. The increase in transverse dimension has two effects on band structure: reduce the band gap; and widen the sharp DOS peaks, both have negative impacts on Seebeck coefficient. So the Seebeck coefficient decreases quickly with transverse size increasing.

In thermoelectric application, the power factor P, which is defined as $P = S^2\sigma$, is an important factor influencing the thermoelectric performance directly. Figure 9 (c) shows the power factor versus carrier concentration for SiNWs with different cross sectional areas. The power factor increases with carrier concentration increases, and there is an optimal carrier concentration N_{Max} yielding the maximum attainable value of P_{Max}. Above N_{Max}, the power factor decreases with increasing carrier concentration. This phenomenon can be understood as below. Increasing carrier concentration has two effects on power factor. On the one hand, the increase of carrier concentration will increase the electrical conductivity. On the other hand, the increase of carrier concentration will suppress the Seebeck coefficient S. The power factor is determined by these two effects that compete with each other. Therefore, there exits an optimal carrier concentration N_{Max}. With SiNW diameter increases, the maximum attainable power factor P_{Max} decreases (as shown in figure 9(c)), due to the slow increase of σ is offset by obvious decreasing in S (P~S^2). Figure 9 (d) shows the maximum power factor P_{Max} versus the cross section area of SiNWs. With the area increases from about 1 nm^2 to 18 nm^2, the maximum power factor decreases from about 6800 to 1400 μW/m-K^2. At small size, the small increases of cross section area can induce large reduction on power factor. For example, with the cross section area increases from 1.1 to 4.7 nm^2, the power factor decreases with about 4300 μW/m-K^2. In contrast to the high sensitivity at the small size range, the power factor versus cross section area curves are almost flat at the large wire range, where the power factor is almost constant when cross section area increases from 14.1 to 17.8 nm^2.

In the calculation of ZT, both electron and phonon contribute to the total thermal conductivity. It is clear that electron thermal conductivity increases with diameter as it is proportional to electronic conductivity. For SiNWs with length in μm scale, the phonon thermal conductivity increases with diameter increases remarkably until the diameter is larger than about hundreds nms. (Liang & B. Li, 2006) As both the electron and phonon contributions to thermal conductivity increase as transverse size increasing, it is obvious that the total thermal conductivity increases with transverse dimension. Combine the size dependence of the power factor as shown in figure 9(d), we can conclude that ZT will decrease when the NW diameter increases.

As we discussed above, the isotope doping is an important method to modulate the thermal conductivity of nano materials. Now we focus on the isotope doping effect on ZT of SiNW ($^{28}Si_{1-x}{}^{29}Si_x$ NWs) with fixed cross section area of 2.3 nm^2. Here we use the phonon thermal conductivity value calculated in (Yang et al., 2008) with cross section area of 2.6 nm^2. It is obvious that within the moderate carrier concentration, the thermal conductivity from phonons is much larger than that from electrons. Using the calculated S, σ, electron thermal conductivity and the phonon thermal conductivity, the dependence of maximum attainable

value of ZT_{Max} on doping concentration is shown in figure 10(a). The ZT_{Max} values increase with ^{29}Si concentration, reach a maximum and then decreases. This phenomenon is from the isotope doping effect on lattice thermal conductivity. (Yang et al., 2008) At low isotopic percentage, the small ratio of isotope atoms can induce large increase in ZT_{Max}. For instance, in the case of $^{28}Si_{0.8}{}^{29}Si_{0.2}$ NW, its ZT_{Max} increases with 15% from that of pure ^{28}Si NW. And with 50% ^{29}Si doping, the ZT_{Max} can increase with 31%.

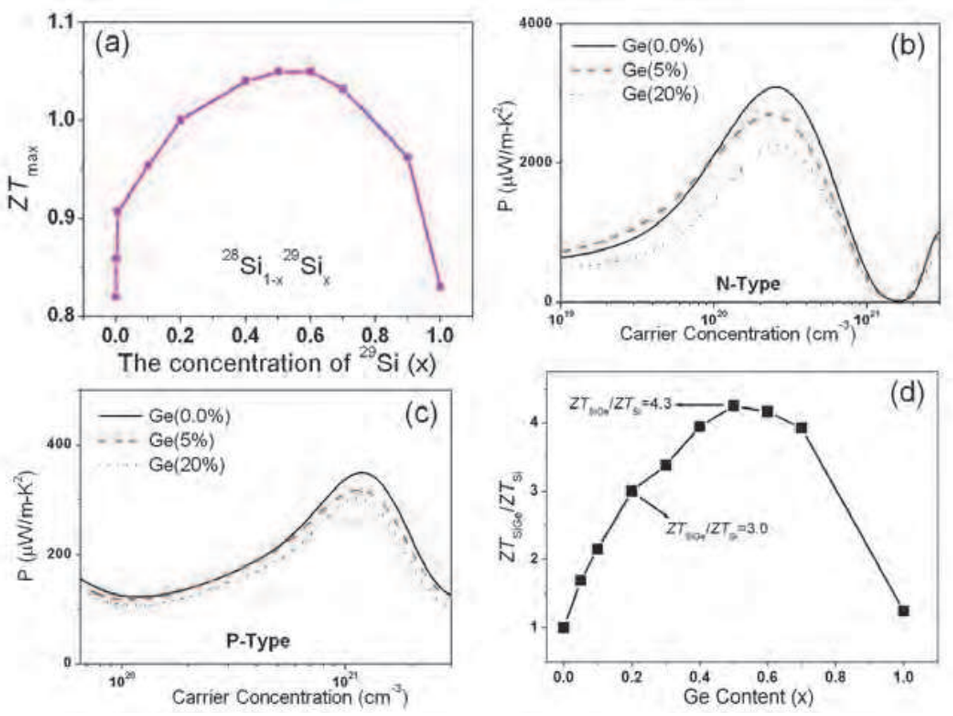

Fig. 10. (a) ZT_{Max} vs the concentration of ^{29}Si atom. Thermal power factors of $Si_{1-x}Ge_x$ NWs versus carrier concentration for n-type wires (b) and p-type wires (c). (d) $ZT_{Si1-xGex}/ZT_{Si}$ versus the Ge content x for n-type $Si_{1-x}Ge_x$ wires.

Besides SiNW, it has also been demonstrated that $Si_{1-x}Ge_x$ NW is a promising candidate for high-performance thermoelectric application since its thermal conductivity can be tuned by the Ge contents (J. Chen et al., 2009). It has been observed experimentally that when the Ge content in the $Si_{1-x}Ge_x$ nanocomposites increases from 5% to 20%, the thermal conductivity decreases obviously. (G. H. Zhu et al., 2009) However, at the same time, the power factor also decreases, and induces uncertainty in the change of figure of merit ZT. The composition dependence of the thermoelectric properties in $Si_{1-x}Ge_x$ NWs have been investigated systematically by Shi et al. (L. Shi et al. 2010) Figure 10 (b) and Figure 10(c) show the power factor versus carrier concentration for n-type and p-type wires. The power factor of p-type wire is much smaller (only about 15%) than that in its n-type counterpart because of the reduced charge mobility in p-type wires. As different doping (p-type or n-type) only have various changes on the electronic property, but the same impact on the lattice vibration, so the phonon thermal conductivity of p-type nanowire should be close to that of n-type wire. Combine the calculated power factor, it is obvious that ZT of n-type wire is about 6-7 times

of that of p-type nanowire. In the next, we only show the Ge content dependent *ZT* of n-type NW. Using the calculated *S*, and σ and the relative phonon thermal conductivity (k_{SiGe}/k_{Si}, here k_{Si} and k_{SiGe} are thermal conductivities of SiNW and $Si_{1-x}Ge_x$ NW, respectively) calculated by using molecular dynamics method from (J. Chen et al., 2009), the dependence of $ZT_{Si1-xGex}/ZT_{Si}$ on Ge content x is shown in figure 10(d). The $ZT_{Si1-xGex}/ZT_{Si}$ values increase with Ge content, reach a maximum and then decreases. It is worth pointing out that the calculated *ZT* of pure Ge NW is only 1.3 times of that of pure SiNW, which is far less that the 9-fold increase in the respective bulk materials. The remarkable difference in the increased factor of *ZT* between the respective bulk and nanowires is due to the similarity of the thermal conductivity and electronic property in the nano scale. Moreover, at low Ge content, the small ratio of Ge atoms can induce large increase in *ZT*. For instance, in the case of $Si_{0.8}Ge_{0.2}$ NW, namely, 20% Ge, $ZT_{Si1-xGex}/ZT_{Si}$ is about 3. And with 50% Ge atoms ($Si_{0.5}Ge_{0.5}$ NW), the $ZT_{Si1-xGex}/ZT_{Si}$ can be as high as 4.3. Combine with the experimental measured *ZT* of n-type SiNW which is about 0.6-1.0, it is exciting that we may obtain high *ZT* value of about 2.5-4.0 in n-type $Si_{1-x}Ge_x$ NW.

7. Realization of SiNW based on-chip coolers

Typical integrated circuit (IC) chips have millions or even billions of transistors, which can generate huge heat fluxes in very small areas which is called as hot-spot. The hot spot removal is a key for future generations of IC chips. Circulated liquid cooling is one of current available cooling technologies, which moves heat sink away from the processors by increasing the surface area. However, reliability is a big concern if the liquid hose is leaking. Moreover, this and other conventional cooling techniques are used to cool the whole package temperature and none of them addresses the hot spots cooling. The hot spots in microprocessors are normally in the order of 300-400 μm in diameter, thus even the smallest commercial cooling module is still too large for spot cooling. In addition, as the three-dimensional (3D) chips are investigated, this can create smaller and hotter spots. The current cooling technologies are fast reaching their limits. High efficiency and nano scale cooler is a key enabler to remove small hot spots in IC chips and for the future improvements of IC thermal management. To solve the hot spot issue, one way is to use thermoelectric (TE) materials to cool the hot spot. In above of this chapter, we have discussed the thermal and thermoelectric properties of NWs. A natural question comes promptly: if a cooler is built from SiNW, then how cool we can achieve? And what are the cooling power and efficiency? In this section, we will show the answers to these questions.

By using finite element simulation, Zhang et al. (G. Zhang et al., 2009a) studied the the cooling temperature, cooling power density and coefficient of performance of SiNW based on-chip cooler. The size of SiNW is 50 nm × 50 nm × 2.5 μm. Upon electrical current flow through, electrons absorb thermal energy from lattice at one junction and transport it to another junction (Peltier effect), creating a cold and hot side. Here the assumed hot spot is in contact with the cold side and the hot side is fixed at 300 K. Besides this positive cooling effect, the back-flow of heat from hot end to cold end and Joule heat will weaken the cooling efficiency. So heat flux is the sum of Seebeck (Peltier) effect, Fourier effects, and the Joule heat. For SiNW with 50 nm diameter, 20 W/m-K is observed for vapour-liquid-solid grown SiNW (VLS-SiNWs), while 1.6 W/m-K is found for aqueous electroless-etching grown wire (EE-SiNWs). (Hochbaum et al., 2008) The large

discrepancy in thermal conductivity lies from the surface scattering of phonons. Both thermal conductivity values are used to explore the importance of thermal conductivity on thermoelectric performance. Natural convection and radiation as the heat transfer mechanism between the system and the surrounding air are established. The surrounding environment is assumed to be stationary air at atmospheric pressure. From the finite element simulation, it was found that for nanoscale systems such as SiNWs, the contribution of natural convection and radiation are very low in the total heat transfer, while thermal conduction is the major contribution. (G. Zhang et al., 2009a)

Figure 11(a) shows the cooling temperature versus electrical current. For both EE-wire and VLS-wire, the cooling temperature increases with supplied current increases, and there is a maximum at about I_M=3.5-4.0 μA. Above I_M, cooling temperature decreases with increasing current. This phenomenon can be understood as below. Increasing electrical current has two effects on cooling. On the one hand, the increase of electrical current will absorb more thermal energy from one end and transport it to another end. We call this effect the "positive" effect. On the other hand, the increase of electrical current will also increase Joule heating that in turn will increase the heat flux to the cool end, thus suppress cooling. We call it the "negative" effect. The cooling temperature is determined by these two effects that compete with each other. And as demonstrated in Figure 11(a), the maximum cooling temperature of EE-wire is much larger than that of VLS-wire, although they are with the same dependence characteristic on electrical current.

In the cooling temperature analysis above, the hot spot is a non-source device. If the device (hot spot) generates heat, the maximum cooling temperature will depend on the dissipation power, and we can predict the maximum cooling power that SiNW cooler can arrive. Fig. 11(b) shows the relation between the cooling temperature with the power dissipation density from the device for both EE- and VLS-SiNWs with electrical current of 4 μA. The maximum cooling power is defined as the heat load power that makes the device's maximum cooling temperature equal to zero. The maximum cooling power density is about 6.6 $\times 10^3$ W/cm^2 here, and is independent on the special thermal conductivity. The independence of maximum cooling power density on thermal conductivity is due to the maximum cooling power is arrived when the temperature difference between the two ends is zero and no Fourier heat flux. The maximum cooling power density, 6.6 $\times 10^3$ W/cm^2 for SiNW, is about six times larger than that of SiGeC/Si superlattice coolers (X. Fan et al., 2001), ten times larger than that of Si/Si_xGe_{1-x} thin film cooler (Y. Zhang et al., 2006), and six hundred times larger than that of commercial TE module. (Rowe 2006)

The performance of any thermoelectric material is in general expressed by its coefficient of performance (COP). This is defined as the actual cooling power divided by the total rate at which electrical energy is supplied. The electrical power consumption of SiNW cooler is used to generate the Joule heat and overcome the Seebeck effect, which generates power due to the temperature difference between the two junctions of the wire. However, the maximum cooling power is the heat load power that makes the device's maximum cooling temperature equal to zero, so here the electrical power consumption is equal to the Joule heat. From Figure. 11, we can obtain the COP for both EE and VLS nanowires are 61%. This is larger than that of Si/Si_xGe_{1-x} thin film cooler (Y. Zhang et al., 2006) which is 36%, and larger than that of commercial TE module which is only 0.1%. (Rowe 2006)

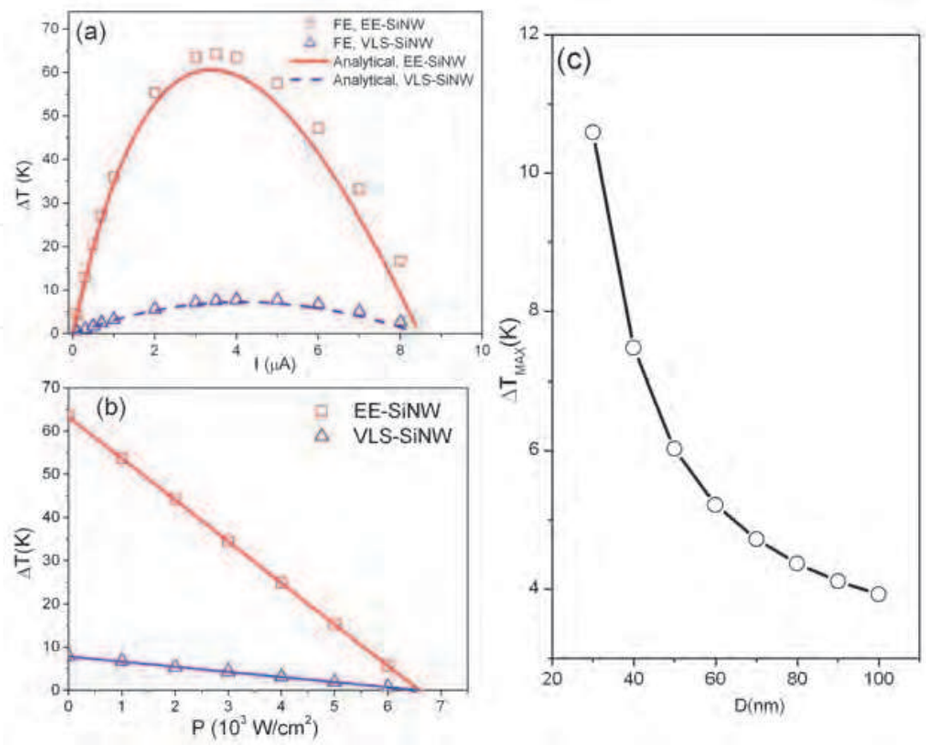

Fig. 11. (a) Dependences of cooling temperature on thermal conductivity and applied electrical current. (b) Cooling temperature versus heat load power density. (c) Maximum cooling temperature vs diameter of SiNW.

From the analytical expression of cooling temperature, we can provide a prediction of the transverse size effect on the cooling temperature. For SiNWs with length in μm scale, the thermal conductivity increases with diameter increases remarkably until the diameter is larger than about hundreds nm. (Liang and B. Li, 2006) Using the quantitative formula for the size-dependent thermal conductivity from Eq. 7, Figure 11(c) shows the maximum cooling temperature vs diameters of SiNWs. It is obvious that cooling temperature decreases as diameter increases. When the diameter increases to 100 nm, the maximum cooling temperature is only about 4K. So to keep high cooling temperature, SiNW with small diameter is preferred.

In the following, we will discuss time dependent cooling performance of SiNWs, (G. Zhang et al., 2009b) including the cooling response time, and the impact of number of SiNWs in the bundle. Figure 12(a) shows the time dependent temperature of the hot spot. Upon current flow through the SiNW, the temperature of the island decreases exponentially initially and then converges to a constant temperature T_C which is much lower than the environment temperature T_0. The cooling temperature $\Delta T=T_0-T_C$. From the best fitting of the time dependent temperature curves, the cooling response time t_0 can be calculated. Figure 12(b) shows that t_0 decreases as applied electrical current increases monotonously. From Figure 12 (a), the maximum cooling temperature can be achieved with about 3-4 μA electrical current, which corresponds to 0.05-0.06 s response time. This demonstrates that SiNW is a fast response cooler.

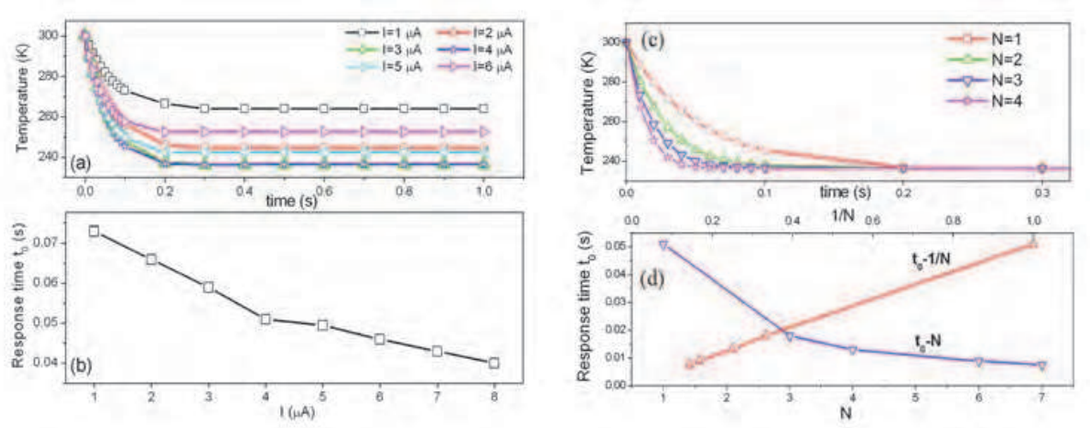

Fig. 12. (a) Time dependent temperature of the hot spot for different applied electrical current. (b) Dependences of cooling response time on applied electrical current. (c) The time dependent temperature for different number of SiNWs *N*. (d) The cooling response time t_0 for different number of SiNWs *N*. Here the electrical current is 4 μA.

In practical application, a bundle of SiNWs will be used, which can be realized by top-down method on SOI wafers. Figure 12 (c) shows the time dependent temperature of the silicon island with a number of SiNWs *N* (>1). With increase in *N*, the cooling process becomes faster. However, the maximum ΔT does not change with *N*. Figure 12 (d) shows the *N* dependent response time. It is obvious that in practical applications, increasing of *N* is an efficient approach to speed the cooling process.

8. Conclusions

The present article tries to give an overview of the thermal and thermoelectric property of semiconducting nanowires. Here we use Silicon nanowires as examples, however, the physics addressed in this article is not limited to silicon system. The thermal transport in low dimensional system has attracted wide research interests in last decade. Silicon Nanowires are promising platforms to verify fundamental phonon transport theories. Moreover, the study of thermal property of SiNWs is also important for potential application, such as waste heat energy harvesting and on-chip cooling. Compared with ten years ago, we have a comprehensive understanding of the impacts of doping, surface scattering and alloy effect on thermal conductance and thermoelectric property of nanowires. However, further experimental and theoretical studies on fundamental mechanism will be greatly helpful to advance the field.

9. Acknowledgment

The authors wish to thank Prof. Baowen Li, Dr. Nuo Yang, Dr. Jie Chen and Dr. Lihong Shi for long time collaboration and support. And acknowledge the support by the Ministry of Science and Technology of China (Grant Nos. 2011CB933001).

10. References

Berber, S.; Kwon, Y.-K. & Tománek, D. (2000) Unusually High Thermal Conductivity of Carbon Nanotubes. *Phys. Rev. Lett.*, Vol. 84, No. 20 (May 2000) pp.4613.

Boukai, A. I.; Bunimovich, Y.; Kheli, J. T.; Yu, J-K.; Goddard III, W. A. & Heath, J. R. (2008) Silicon nanowires as efficient thermoelectric materials. *Nature*, Vol. 451, No.7175, (January 2008), pp. 168-172.

Bourgeois, O.; Fourniew, T. & Chaussy, J. (2007), Measurement of the thermal conductance of silicon nanowires at low temperature. *Journal of Applied Physics*, Vol. 101, No. 1 (January 2007) pp. 016104-016106.

Cahill, D. G.; Ford, W. K.; Goodson, K. E. *et al.* (2002) Nanoscale thermal transport, *J. Appl. Phys.*, Vol. 93, No. 2, (August 2002), pp. 793-818.

Che, J.; Cagın, Tahir; Deng, W. & Goddard III, W.A. (2000) Thermal conductivity of diamond and related materials from molecular dynamics simulations, *J. Chemical Physics*, Vol. 113, No. 16 (July 2000) pp.6888-6900.

Chen, J.; Zhang, G. & Li, B., (2009), Tunable Thermal Conductivity of $Si_{1-x}Ge_x$ Nanowires, Appl. Phys. Lett. Vol. 95, No. 7 (August 2009), pp. 073117.

Cui, Y.; Wei, Q.; Park, H. & Lieber, C. M. (2001) Nanowire Nanosensors for Highly Sensitive and Selective Detection of Biological and Chemical Species, *Science*, Vol. 293, (August 2001), pp. 1289-1292.

Donadio, D. & G. Galli, (2009) Atomistic Simulations of Heat Transport in Silicon Nanowires, *Phys. Rev. Lett.*, Vol. 102, No. 19 (May 2009) pp. 195901.

Fan, X.; Zeng, G.; Labounty, C.; Bowers, J. E.; Croke, E.; Ahn, C. C.; Huxtable, S.; Majumdar, A. & Shakouri, A. (2001) SiGeC/Si superlattice microcoolers, Appl. Phys. Lett. Vol. 78, No. 11 (January 2001) pp. 1580.

Gilbert, M. J.; Akis, R. & Ferry, D. K. (2005), Phonon-assisted ballistic to diffusive crossover in silicon nanowire transistors, *J. Appl. Phys.*, Vol. 98, No. 9, (November 2005) pp. 094303-094310.

Hochbaum, A. I.; Chen, R.; Delgado, R. D.; Liang, W.; Garnett, E. C.; Najarian, M.; Majumdar, A. & Yang, P. (2008) Enhanced thermoelectric performance of rough silicon nanowires, *Nature*, Vol. 451, No. 7175, (January 2008), pp. 163-168.

Iijima, S. (1991) Helical microtubules of graphitic carbon. *Nature* Vol. 354, No. 6345 (November 1991) pp. 56 - 58.

Kim, P.; Shi, L.; Majumdar, A. & McEuen, P. L. (2001) Thermal Transport Measurements of Individual Multiwalled Nanotubes. *Phys. Rev. Lett.*, Vol. 87, No. 21 (October 2001), pp. 215502.

Li, B. & Wang, J. (2003), Anomalous Heat Conduction and Anomalous Diffusion in One-Dimensional Systems, *Phys. Rev. Lett.* Vol. 91, No. 4 (July 2003) pp. 044301.

Li, B.; Wang, J.; Wang, L. & Zhang, G. (2005) Anomalous heat conduction and anomalous diffusion in nonlinear lattces, single wall nanotubes, and billiard gas channels. *Chaos*, Vol. 15, No. 1, (April, 2005), pp. 015121

Li, D.; Wu, Y.; Kim, P.; Shi, L.; Yang, P. & Majumdar, A. (2003) Thermal conductivity of individual silicon nanowires, *Appl. Phys. Lett.*, Vol.83, No. 14 (August 2003) pp. 2934.

Li, J.; Yu, H.; Wong, S.; Li, X.; Zhang, G.; Lo, G-Q & Kwong, D.-L., (2009) Design guidelines of periodic Si nanowire arrays for solar cell application. *Appl. Phys. Lett.*, Vol. 95, No. 24 (December 2009) pp. 243113.

Liang, L. H. & Li, B. (2006) Size-dependent thermal conductivity of nanoscale semiconducting systems, *Phys. Rev. B*, Vol. 73, No. 15, (April 2006) pp. 153303.

Maruyama, S. (2002) A Molecular Dynamics Simulation of Heat Conduction of Finite Length SWNTs, *Physica B*, Vol. 323, No. 1-4 (October 2002), pp. 193-195.

Moutanabbir, O.; Senz, S.; Zhang, Z. & Gösele, Ulrich (2009), Synthesis of isotopically controlled metal-catalyzed silicon nanowires. *Nano Today*, Vol. 4, No. 5 (August 2009), pp. 393-398.

Park, M.; Kim, M.; Joo, J.; Kim, K.; Kim, J.; Ahn, S.; Cui, Y. & Cho, J. (2009) Silicon Nanotube Battery Anodes, *Nano Lett.*, Vol. 9, No. 11 (November 2009) pp. 3844-3847.

Rowe, D. M. (2006). *Thermoelectrics Handbook Macro to Nano*, Taylor & Francis Group, France.

Shi, L.; Yao, D.; Zhang, G. & Li, B. (2009) Size Dependent Thermoelectric Properties of Silicon Nanowires, *Appl. Phys. Lett.*, Vol. 95, No. 6 (August 2009) pp. 063102.

Shi, L.; Yao, D.; Zhang, G. & Li, B. (2010) Large Thermoelectric Figure of Merit In $Si_{1-x}Ge_x$ Nanowires, *Appl. Phys. Lett.*, Vol. 96, No. 17 (April 2010) pp. 173108.

Stillinger, F. H. & Weber, T. A. (1985) Computer simulation of local order in condensed phases of silicon. Phys. Rev. B, Vol. 31, No. 8, (April 1985) pp. 5262-5271.

Volz, S. G. & Chen, G., (1999) Molecular dynamics simulation of thermal conductivity of silicon nanowires, *Appl. Phys. Lett.*, Vol. 75, No. 14 (August 1999) pp. 2056.

Volz, S. G. & Chen, G. (2000), Molecular-dynamics simulation of thermal conductivity of silicon crystals, *Phys. Rev. B*, Vol. 61, No. 4 (January 2000) pp. 2651-2656.

Wang, R. Y.; Feser, J. P.; Lee, J-S; Talapin, D. V.; Segalman, R. & Mujumdar, A. (2008) Enhanced Thermopower in PbSe Nanocrystal Quantum Dot Superlattices, *Nano Lett.*, Vol. 8, No. 8 (August 2008) pp. 2283-2288.

Wang, X.; Shakouri, A.; Yu, B.; Sun, X. & Meyyappan, M. (2007) Study of phonon modes in germanium nanowires, *Journal of Applied Physics*, Vol. 102, No. 1 (July 2007), pp. 014304-014309.

Xiang, J,; Lu, W,; Hu, Y,; Wu, Y,; Yan, H, & Lieber, C. M. (2006), Ge/Si nanowire heterostructures as high-performance field-effect transistors. *Nature*, Vol. 441, No. 7092,(May, 2006) pp. 489-494.

Yamamoto, T.; Watanabe, S. & Watanabe, K.(2004), Universal Features of Quantized Thermal Conductance of Carbon Nanotubes. *Phys. Rev. Lett.*, Vol. 92, No. 7 (February 2004), pp.075502.

Yang, J-E.; Jin, C-B.; Kim, C-J. & Jo, M-H. (2006), Band-Gap Modulation in Single-Crystalline $Si_{1-x}Ge_x$ Nanowires, Nano Lett., Vol. 6, No. 12 (December 2006) pp. 2679-2684.

Yang, N.; Zhang, G. & Li, B. (2008), Ultralow Thermal Conductivity of Isotope-Doped Silicon Nanowires. *Nano Letters*, Vol. 8, No. 1 (January, 2008) pp. 276-280.

Yang, N.; Zhang, G. & Li, B. (2010), Violation of Fourier's Law and Anomalous Heat Diffusion in Silicon Nanowires. *Nano Today*, Vol. 5, No. 2 (March 2010) pp. 85-90.

Zhang, G. & Li, B. (2005) Thermal conductivity of nanotubes revisited: Effects of chirality, isotope impurity, tube length, and temperature. *J. Chem. Phys.*, Vol. 123, No. 114714. (September 2005), pp. 114714.

Zhang, G.; Zhang, Q. X.; Bui, C.-T.; Lo, G.-Q. & Li, B. (2009) Thermoelectric Performance of Silicon Nanowires, *Appl. Phys. Lett.*, Vol. 94, No. 21 (May 2009) pp. 213108.

Zhang, G.; Zhang, Q.-X.; Kavitha, D. & Lo, G.-Q. (2009) Time Dependent Thermoelectric Performance of A Bundle of Silicon Naowires For On-Chip Cooler Applications, *Appl. Phys. Lett.*, Vol. 95. No. 24, (December 2009) pp. 243104.

Zhang, G. & Li, B. (2010), Impacts of Doping On Thermal And Thermoelectric Properties of Nanomaterials. *NanoScale*, Vol. 2, No. 7 (July 2010), pp. 1058-1068.

Zhang, Y.; Christofferson, J.; Shakouri, A.; Zeng, G.; Bowers, J. E. & Croke, E. T. (2006) On-chip high speed localized cooling using superlattice microrefrigerators, *IEEE Transactions on Components and Packaging Technologies*, Vol. 29, No. 2, (June 2006). pp. 395-401.

Zhu, G. H.; Lee, H.; Lan, Y.C.; Wang, X.W.; Joshi, G.; Wang, D.Z.; Yang, J.; Vashaee, D.; Guilbert, H.; Pillitteri, A.; Dresselhaus, M.S.; Chen, G. & Ren, Z.F. (2009) Increased Phonon Scattering by Nanograins and Point Defects in Nanostructured Silicon with a Low Concentration of Germanium. *Phys. Rev. Lett.*, Vol. 102, No. 19 (May 2009) pp. 196803.

Nanowires - Fundamental Research

Edited by Dr. Abbass Hashim

ISBN 978-953-307-327-9
Hard cover, 552 pages
Publisher InTech
Published online 19, July, 2011
Published in print edition July, 2011

Understanding and building up the foundation of nanowire concept is a high requirement and a bridge to new technologies. Any attempt in such direction is considered as one step forward in the challenge of advanced nanotechnology. In the last few years, InTech scientific publisher has been taking the initiative of helping worldwide scientists to share and improve the methods and the nanowire technology. This book is one of InTechâ€™s attempts to contribute to the promotion of this technology.

How to reference

In order to correctly reference this scholarly work, feel free to copy and paste the following:

Gang Zhang (2011). Nanowire Applications: Thermoelectric Cooling and Energy Harvesting, Nanowires - Fundamental Research, Dr. Abbass Hashim (Ed.), ISBN: 978-953-307-327-9, InTech, Available from: http://www.intechopen.com/books/nanowires-fundamental-research/nanowire-applications-thermoelectric-cooling-and-energy-harvesting

INTECH
open science | open minds

InTech Europe
University Campus STeP Ri
Slavka Krautzeka 83/A
51000 Rijeka, Croatia
Phone: +385 (51) 770 447
Fax: +385 (51) 686 166
www.intechopen.com

InTech China
Unit 405, Office Block, Hotel Equatorial Shanghai
No.65, Yan An Road (West), Shanghai, 200040, China
中国上海市延安西路65号上海国际贵都大饭店办公楼405单元
Phone: +86-21-62489820
Fax: +86-21-62489821

IntechOpen